

# <sup>35</sup>Cl NQR, <sup>1</sup>H NMR, and X-Ray Diffraction Studies in a Hydrogen Bonded Complex Na<sub>2</sub>PtCl<sub>6</sub> · 6H<sub>2</sub>O\*

Hiroshi Miyoshi, Keizo Horiuchi<sup>a</sup>, Narumi Sakagami, Kenichi Okamoto, and Ryuichi Ikeda

Department of Chemistry, University of Tsukuba, Tsukuba 305, Japan

<sup>a</sup> College of Science, University of the Ryukyus, Senbaru, Nishihara, Okinawa 903-01, Japan

Z. Naturforsch. **53a**, 603–607 (1998); received October 31, 1997

The <sup>35</sup>Cl NQR frequencies, spin-lattice relaxation time and <sup>1</sup>H NMR relaxation time were measured on crystalline Na<sub>2</sub>PtCl<sub>6</sub> · 6H<sub>2</sub>O at 77–350 K. The presence of three nonequivalent chlorine sites found by X-ray diffraction measurement is in agreement with the observed three NQR lines, which have different temperature dependences attributable to differences in the direction of H-bonding with water molecules. The three NQR lines correspond to three kinds of chlorines with different Pt–Cl distances and H-bond directions.

**Key words:** Cl NQR; X-Ray Diffraction; Spin-Lattice Relaxation; Quadrupole Coupling Constant; Hydrogen Bond.

## 1. Introduction

Halogen NQR frequencies and their variation with temperature are sensitive probes for detecting hydrogen bonds X ··· H and their temperature dependence [1]. They can clearly indicate the change of the electric-field-gradient around the halogen nuclei due to the formation or break of hydrogen bonds [2, 3].

In the present study we investigate the effect of Cl ··· H<sub>2</sub>O-type H-bonding on NQR frequencies and its relaxation time in Na<sub>2</sub>PtCl<sub>6</sub> · 6H<sub>2</sub>O crystals from <sup>35</sup>Cl NQR and single crystal X-ray diffraction studies.

## 2. Experimental

Na<sub>2</sub>PtCl<sub>6</sub> · 6H<sub>2</sub>O was prepared by mixing commercial H<sub>2</sub>PtCl<sub>6</sub> · 6H<sub>2</sub>O dissolved in water and an equivalent amount of NaCl dissolved in hydrochloric acid, and evaporating the solvent in a desiccator over P<sub>2</sub>O<sub>5</sub>. The obtained crystals were recrystallized from hydrochloric acid.

<sup>35</sup>Cl NQR signals were observed with a home-made pulsed spectrometer consisting of an Anritsu MG3601A signal generator, a Thamway P10-6704 phase shifter, an R&K A8520-RS rf power amplifier, a

Matec Model 252 preamplifier, and an Iwatsu DS-9121 digital oscilloscope. We observed echo signals by applying a  $\pi/2 - \tau - \pi$  pulse sequence. The sample temperature was controlled by a Chino Model SU temperature controller within  $\pm 1$  K, and determined by a chromel – constantan thermocouple.

The <sup>35</sup>Cl NQR spin-lattice relaxation time  $T_{1Q}$  was measured by use of a  $\pi - \tau - \pi/2$  pulse sequence and the height of FID signals was plotted against the time interval  $\tau$ .

The <sup>1</sup>H NMR spin-lattice relaxation time  $T_{1H}$  was measured by a Bruker SXP100 pulsed spectrometer at a Larmor frequency of 42 MHz using the saturation recovery method.

Single crystal X-ray diffraction measurements were performed at room temperature using an Enraf Nonius CAD4 diffractometer with a graphite-monochromated MoK $\alpha$  radiation ( $\lambda = 71.073$  pm) at room temperature.

## 3. Results and Discussion

### 3.1 X-Ray Structure Analysis

An orange crystal (0.08 × 0.23 × 0.50 mm) of the compound was used for data collection. Unit cell dimensions were obtained from a least-squares refinement, using the setting angles of 25 reflections in the range  $8 < 2\theta < 21^\circ$ . Crystal data: Na<sub>2</sub>PtCl<sub>6</sub> · 6H<sub>2</sub>O, M.W. = 561.88, triclinic,  $P\bar{1}$  (No. 2),  $a = 674.58(5)$ ,  $b = 709.7(1)$ ,  $c = 837.56(8)$  pm,  $\alpha = 101.99(1)$ ,  $\beta = 98.725(9)$ ,  $\gamma =$

\* Presented at the XIVth International Symposium on Nuclear Quadrupole Interactions, Pisa, Italy, July 20–25, 1997.

Reprint requests to Prof. Ryuichi Ikeda,  
Fax: + 812 98 53 65 03, e-mail: ikeda@staff.chem.tsukuba.ac.jp



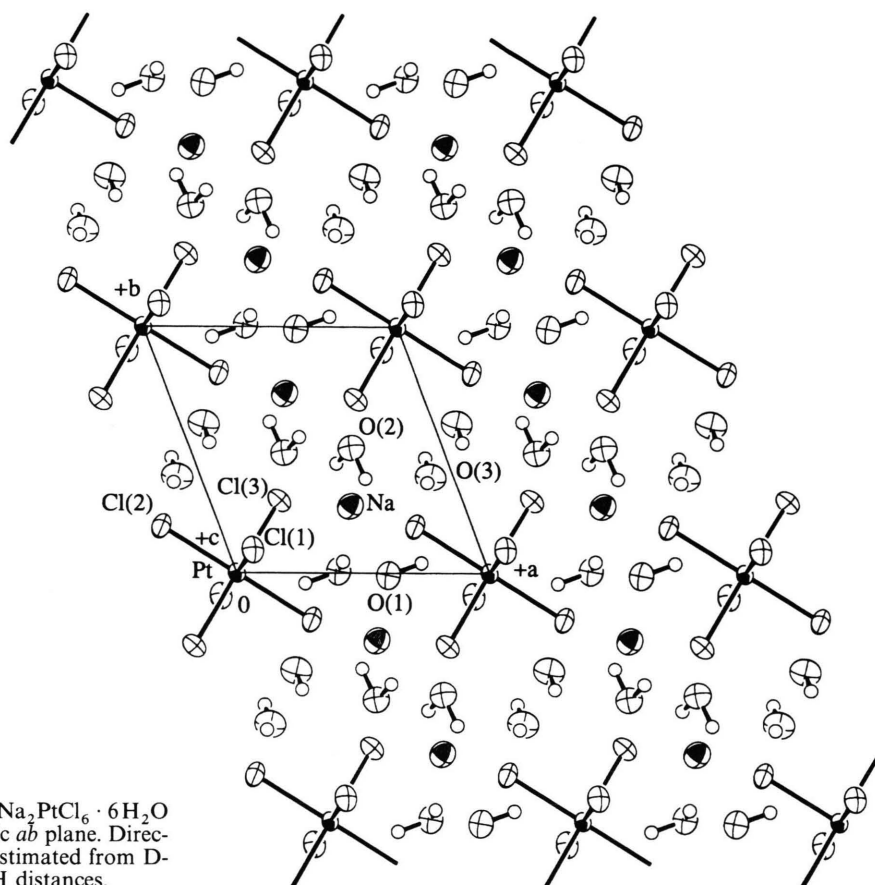


Fig. 1. The ORTEP diagram of  $\text{Na}_2\text{PtCl}_6 \cdot 6\text{H}_2\text{O}$  projected on the crystallographic  $ab$  plane. Directions of hydrogen atoms were estimated from D-Fourier map by fixing the O–H distances.

$108.238(7)^\circ$ ,  $V = 3.6228(9) \times 10^8 \text{ pm}^3$ ,  $Z = 1$ ,  $D_c = 2.575 \text{ g cm}^{-3}$ ,  $F(000) = 262$ ,  $\mu(\text{MoK}\alpha) = 108.08 \text{ cm}^{-1}$ . Of 2346 reflections 2185 were unique. The structure was solved by direct methods and expanded using Fourier technique. The non-hydrogen atoms were refined anisotropically. All hydrogen atom coordinates were refined by the fixed O–H distance (95 pm and thermal constraints ( $u = 1.2 u(0)$ ). The final cycle of full-matrix least-squares refinement on  $F$  was based on 1826 reflections ( $I > 2\sigma(I)$ ):  $R = 0.053$ ,  $R_w = 0.060$ . The calculations were performed using the teXsan crystallographic software package of Molecular Structure Corporation. The determined atomic coordinates are shown in Table 1.

Figure 1 shows an ORTEP diagram projected on the crystallographic  $ab$  plane, where Pt atoms are located on the inversion centre implying that the two Cl atoms in the trans positions are equivalent. The chlorine atoms associated with three kinds of Pt–Cl bonds with distances of 232.0(4), 231.9(5) and 233.2(4) pm

Table 1. Final atomic coordinates and equivalent isotropic thermal parameters ( $B_{\text{eq}}/\text{pm}^2 \times 10^{-4}$ )\*.

Atom	<i>x</i>	<i>y</i>	<i>z</i>	$B_{\text{eq}}$
Pt	0.000	0.000	0.000	1.80(1)
Cl(1)	−0.2266(7)	0.1866(7)	0.0122(6)	2.82(8)
Cl(2)	0.0966(7)	0.0922(7)	0.2912(5)	2.67(8)
Cl(3)	0.2740(7)	0.2942(7)	−0.0033(6)	2.77(8)
Na	0.455 (1)	0.731 (1)	0.479 (1)	3.6 (2)
O(1)	0.404 (2)	0.011 (2)	0.659 (2)	3.6 (3)
O(2)	0.365 (2)	0.492 (2)	0.645 (2)	3.6 (3)
O(3)	0.092 (3)	0.608 (3)	0.316 (2)	4.3 (4)

\*  $B_{\text{eq}} = (8\pi^2/3) \sum \sum U_{ij} a_i^* a_j^* a_i \cdot a_j$

are shown as Cl<sub>(1)</sub>, Cl<sub>(2)</sub> and Cl<sub>(3)</sub>, respectively, in the figure.

### 3.2 $^{35}\text{Cl}$ NQR Frequencies and Relaxation

We observed three  $^{35}\text{Cl}$  NQR lines with almost the same intensity in the temperature range 77–350 K.

The observed frequencies of  $\nu_1 = 27.081$ ,  $\nu_2 = 26.483$ , and  $\nu_3 = 25.721 \pm 0.002$  MHz at 275 K correspond well to the values reported for room temperature [4]. This result implies that there exist three kinds of crystallographically nonequivalent chlorine atoms, in good agreement with the structural analysis given above. It has been reported from the comparison of halogen NQR frequencies and crystal data [5, 6] that short bond distances arising from a strong covalent bond can be ascribed to the high NQR frequency lines. We may apply this rule to the present data, i.e., Cl(1) and Cl(2) with almost the same Pt–Cl distances can be ascribed to the high frequency lines  $\nu_1$  and  $\nu_2$  or vice versa, and Cl(3) with the longest length to the lowest  $\nu_3$  line.

Upon heating from 77 K, all frequencies decreased almost linearly but with different temperature coefficients up to room temperature as shown in Figure 2. To see their temperature dependences more precisely, frequency differences from values observed at 350 K were plotted in Fig. 3 in which, as a reference, we show the reported temperature dependence of the  $^{35}\text{Cl}$  frequency in  $\text{K}_2\text{PtCl}_6$  [7]. The highest-frequency line  $\nu_1$  has a larger temperature coefficient than those of the lines  $\nu_2$  and  $\nu_3$ , which have coefficients close to that in  $\text{K}_2\text{PtCl}_6$ .

Figure 1 shows that  $\text{Na}^+$  ions are closely surrounded (within ca. 240 pm) by O atoms of water molecules, indicating the presence of strong electrostatic attraction between  $\text{Na}^+$  and O. On the other hand, Cl–H–O type H-bonding is formed because there are short Cl–O distances of 330–360 pm which are shorter than the sum of the van der Waals radii of Cl and H atoms and the O–H bond distance ((120 + 180 + 100) pm).

Since the valence electrons in Cl atom are attracted by H atoms when a Cl–H type hydrogen bond is formed, electrons in the  $p_z$  orbital in Cl partly move to H if the Cl–H bond is nearly along the direction of the Pt–Cl bond, while Cl  $p_x$  or  $p_y$  electrons are pulled, if the H-bond is perpendicular to the Pt–Cl bond. From the simple Townes–Dailey analysis [8], we can see that the resonance frequency increases when an H-bond along Pt–Cl bond is formed, whereas it decreases for the perpendicular H-bonding. In the former case, the observed frequency is expected to decrease rapidly upon heating because the formed H-bond is gradually weakened by thermal vibrations with increasing temperature. On the other hand, the opposite behaviour of frequency will be observed in the latter type of

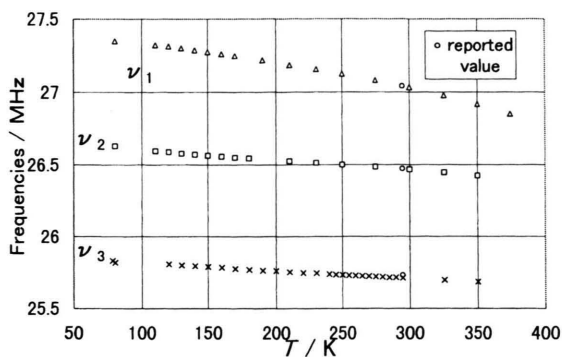


Fig. 2. Temperature dependences of  $^{35}\text{Cl}$  NQR resonance frequencies observed in  $\text{Na}_2\text{PtCl}_6 \cdot 6\text{H}_2\text{O}$ .

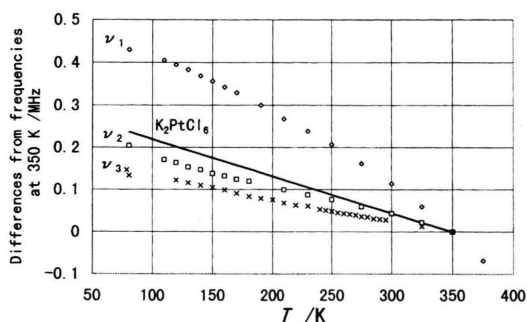


Fig. 3. NQR frequency differences from the values observed at 350 K in  $\text{Na}_2\text{PtCl}_6 \cdot 6\text{H}_2\text{O}$ . The solid line is reported for  $\text{K}_2\text{PtCl}_6$  [7].

H-bond, namely the temperature gradient of frequencies becomes small or sometimes positive.

In Fig. 4, we show the arrangements of oxygen atoms around the three kinds of Cl atoms within distances shorter than 380 pm together with Pt–Cl–O angles. Since accurate H positions are unavailable, we try a rough evaluation of effects of H-bond to NQR data using Cl–O distances and Pt–Cl–O angles. In Fig. 4, short Cl–O distances in nearly the Pt–Cl bond direction are seen for Cl(1), while almost all O atoms are located roughly perpendicular to this direction for Cl(2) and Cl(3). From these results it seems reasonable to assign the line  $\nu_1$  with the largest temperature coefficient to Cl(1), and  $\nu_2$  and  $\nu_3$  to Cl(2) or Cl(3), where we cannot say the correspondence for the latter two. This result is consistent with the previous assignment of the frequencies based on the Pt–Cl bond distances, and Cl(1), Cl(2) and Cl(3) can be most probably assigned to  $\nu_1$ ,  $\nu_2$  and  $\nu_3$ , respectively.

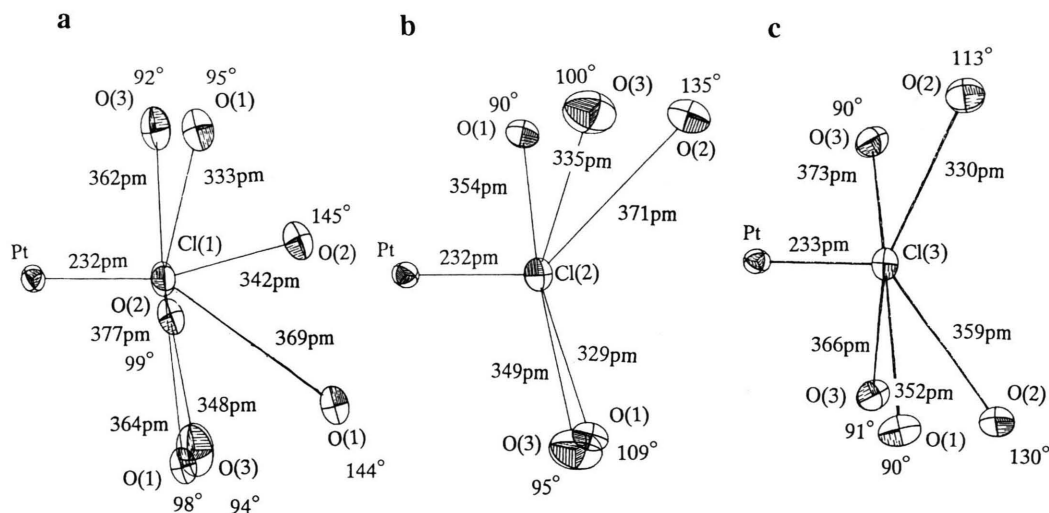


Fig. 4. Arrangement of oxygen atoms in water molecules around resonant  $^{35}\text{Cl}$  nuclei (a: Cl (1), b: Cl (2), and c: Cl (3)).

In Fig. 5 the temperature dependence of the  $^{35}\text{Cl}$  NQR spin-lattice relaxation time  $T_{1Q}$  of the line  $\nu_2$  is shown. The other two lines showed quite analogous temperature dependences. The observed  $T_{1Q}$  gradually decreased upon heating from 77 K, and this behaviour can roughly be fitted to  $T^{-2}$ , as shown in the figure. This relaxation is probably assignable to the effects of rotational vibrations of  $[\text{PtCl}_6]^{-2}$  ions [7].

Around room temperature,  $T_{1Q}$  steeply decreased on heating. This can be explained by an exponential decrease expressed as  $T_{1Q}^{-1} \propto \exp(-E_a/RT)$  due to the onset of reorientations of the whole complex anions [7]. We roughly evaluated the activation energy of this motion as  $E_a = 69 \pm 10 \text{ kJ mol}^{-1}$ . This value is comparable to  $78.6 \text{ kJ mol}^{-1}$  reported for the same motion in  $\text{K}_2\text{PtCl}_6$  [7]. This result implies that the  $\text{Cl}-\text{H}_2\text{O}$  hydrogen bonding is not strong enough for preventing the anionic reorientation.

In these  $T_{1Q}$  data we observed a shallow minimum around room temperature, which could be attributed to some motion of water molecules. To obtain more information about this relaxation process, we measured the  $^1\text{H}$  NMR spin-lattice relaxation time  $T_{1H}$  at 42 MHz. The observed  $T_{1H}$  temperature dependence shown in Fig. 6 exhibits a clear decrease from ca. 200 K with increasing temperature and shows a minimum around room temperature, indicating the onset of a motion of water molecules. By applying the BPP

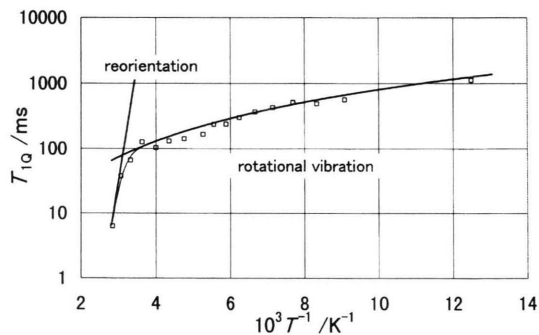


Fig. 5. Temperature dependence of the  $^{35}\text{Cl}$  NQR relaxation time  $T_{1Q}$  observed for the  $\nu_2$  line in  $\text{Na}_2\text{PtCl}_6 \cdot 6\text{H}_2\text{O}$ . Solid lines are fitted theoretical values.

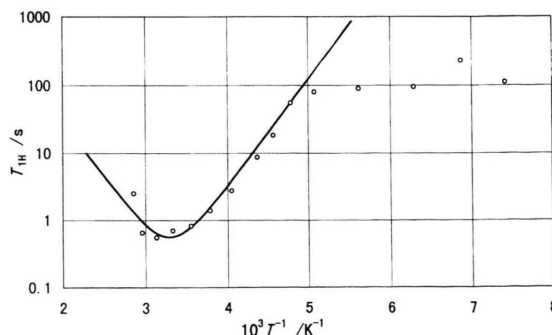


Fig. 6.  $^1\text{H}$  NMR spin lattice relaxation time  $T_{1H}$  observed at 42 MHz in  $\text{Na}_2\text{PtCl}_6 \cdot 6\text{H}_2\text{O}$ . The solid line gives the best-fitted calculated values.

theory [9], we evaluated an activation energy of  $30.2 \pm 1 \text{ kJ mol}^{-1}$  for this motion. The shallow  $T_{1\text{H}}$  minimum value of ca. 0.55 s implies that this motion results in a slight averaging of magnetic dipolar interactions. We attributed this motion to the  $180^\circ$ -flip motion of  $\text{H}_2\text{O}$  contributing only to inter-molecular dipolar relaxation. This assignment is supported by the reported  $T_{1\text{H}}$  data [10, 11] explained by this mo-

tion, which showed minimum values close to the present value.

#### Acknowledgements

This work was partly supported by grant-in-aid for Scientific Research (A) No. 08554027 and (B) No. 09440234 from the Ministry of Education, Science, Sports and Culture, Japan.

- [1] D. Nakamura, R. Ikeda, and M. Kubo, *Coord. Chem. Rev.* **17**, 281 (1975).
- [2] H. Honda, A. Sasane, K. Miyagi, A. Ishikawa, and Y. Mori, *Z. Naturforsch.* **49a**, 209 (1994).
- [3] A. Ishikawa, A. Sasane, Y. Hirakawa, and Y. Mori, *Z. Naturforsch.* **51a**, 693 (1996).
- [4] K. Ito, D. Nakamura, and M. Kubo, *Bull. Chem. Soc. Japan.* **35**, 518 (1962).
- [5] Al. Weiss and S. Wigand, *Z. Naturforsch.* **45a**, 195 (1990).
- [6] Al. Weiss, *Acta Cryst.*, **B51**, 523 (1995).
- [7] K. R. Jeffrey and R. L. Armstrong, *Phys. Rev.* **174**, 359 (1968).
- [8] F. Seitz and D. Turnbull eds., *Solid State Physics*, Suppl. 1, T. P. Das, and E. L. Hahn, "Nuclear Quadrupole Resonance Spectroscopy", Academic Press, New York 1958.
- [9] A. Abragam, *The Principles of Nuclear Magnetism*, Oxford University Press, Oxford 1961.
- [10] R. J. C. Brown, B. K. Hunter, M. Mackowiak, and S. Segel, *J. Magn. Reson.* **50**, 28 (1982).
- [11] A. Sasane, M. Shinha, Y. Hirakawa, and Y. Mori, *J. Mol. Struc.* **345**, 205 (1995).